Effect of Hydrogen incorporation on the mechanical properties of DLC films deposited by HiPIMS in DOMS mode

Costa, A.; Ferreira, Fabio; Colaux, Julien; Vahidi, A.; Serra, R.; Oliveira, J.

Published in:
Surface and Coatings Technology

DOI:
10.1016/j.surfcoat.2023.129980

Publication date:
2023

Document Version
Publisher's PDF, also known as Version of record

Surface & Coatings Technology 473 (2023) 129980

Contents lists available at ScienceDirect

Surface & Coatings Technology

journal homepage: www.elsevier.com/locate/surfcoat

Effect of hydrogen incorporation on the mechanical properties of DLC films deposited by HiPIMS in DOMS mode

A. Costa [a], F. Ferreira [a,b,*], J.L. Colaux [c], A. Vahidi [a], R. Serra [a], J. Oliveira [a]

[a] University of Coimbra, CEMMPRE Centre for Mechanical Engineering Materials and Processes, Department of Mechanical Engineering, Rua Luís Reis Santos, 3030-788 Coimbra, Portugal
[b] LED&Mat-IPN, Instituto Pedro Nunes, Laboratório de Ensaios Desgaste e Materiais, Rua Pedro Nunes, 3030-199 Coimbra, Portugal
[c] Namur Institute of Structured Matter (NISM), Synthesis, Irradiation and Analysis of Materials Platform (SIAM), University of Namur, 5000 Namur, Belgium

ARTICLE INFO

Keywords:
DLC
Hydrogen
HiPIMS
DOMS
Mechanical properties
Tribology

ABSTRACT

The automobile industry has increased its efforts in reducing the emissions of internal combustion engines by improving their efficiency. Decreasing the energy losses by friction in the engines parts is at the core of this attempt. One of the technologies that have been applied in achieving this is the application of carbon coating in engine parts surfaces because of their low friction coefficient characteristics. In this study, DLC films, a specific type of carbon coatings, were deposited using the Deep oscillation magnetron sputtering (DOMS) method, which is a variation of the high-power impulse magnetron sputtering (HiPIMS) method. Those films were deposited with an increasingly higher hydrogen content, and then their mechanical, morphological, and tribological properties were studied. All of this was carried out to verify if the higher hydrogen content is beneficial to use as piston ring coatings in order to decrease friction losses. The variation in the hydrogen content was achieved by increasing the partial pressure of methane inside the deposition chamber during the deposition, which allowed the deposition of films with up to 30 at. % of hydrogen. The variation allowed the depositions of films with a hardness above 10 GPa, a friction coefficient lower than 0.16 (30 % lower when compared to hydrogen-free DLCs), and with specific wear rates in the order of 10^{-16} mm^3/Nm. The hydrogen content also changed the morphology of the films' surface, as well as increasing its deposition rates by 27 %.

1. Introduction

In recent years, the fight against energy losses due to friction has been a constant worry in engineering fields. This battle is crucial to the automobile industry due to the recent efforts in increasing engine efficiency to reduce carbon dioxide emissions. In a regular car, a large percentage of the generated energy is lost due to friction (almost one-third, [1]) in the various moving parts of the engine. So, the scientific community has been committed to finding new ways to reduce these losses, whether through new solid lubricants, new surface textures, or new kinds of surface coatings. Some types of diamond-like carbon (DLC) films are at the core of this constant search, not only for their high hardness but also for their smooth surface, low friction, and high wear resistance [2–7]. DLC films are classified as a random network of sp^3 and sp^2 carbon, with the presence of hydrogen atoms in the case of hydrogenated DLCs [8].

The energy and flux of the depositing species can influence the proportion of sp^3 to sp^2 bonds in DLC films [2,9,10]. For instance, the energy of the depositing species can be adjusted by introducing a bias potential to the substrate if the depositing flux is in the form of ions, making energy control considerably easy.

Ionised physical vapor deposition methods (IPVD) are physical vapor deposition (PVD) techniques where the depositing species' ionised flux percentage is greater than 50 % [11]. Examples of such technologies that generate highly ionised (up to 100 %) deposition flux and hence enhance the formation of sp^3-rich DLC films include cathodic vacuum arc (CVA) and pulsed laser deposition methods (PLD) [2]. Even though these methods offer a highly ionised deposition flux and good film adhesion to substrates, there are some disadvantages of using them, such as the ejection of macroparticles from the target that affect the quality of the films, a lack of lateral uniformity in the film, and difficulty scaling up [3]. DLCs can also be produced by using magnetron sputtering-based techniques. Two popular variations of these techniques are direct current magnetron sputtering (DCMS) and radio frequency magnetron

* Corresponding author at: LED&Mat-IPN, Instituto Pedro Nunes, Laboratório de Ensaios Desgaste e Materiais, Rua Pedro Nunes, 3030-199 Coimbra, Portugal.
E-mail address: fabio.ferreira@dem.uc.pt (F. Ferreira).

https://doi.org/10.1016/j.surfcoat.2023.129980
Received 1 July 2023; Received in revised form 29 August 2023; Accepted 31 August 2023
Available online 1 September 2023

sputtering (RFMS). However, magnetron sputtering-based techniques do not offer significantly ionised deposition fluxes, making it challenging to synthesise dense and sp^3-rich DLC films using these techniques [2,11]. High power impulse magnetron sputtering (HiPIMS) is a magnetron sputtering-based technique created by Kouznetsov et al. [12] that offers a higher ionised deposition flux in comparison to other magnetron sputtering techniques. The use of HiPIMS can produce extremely ionised deposition fluxes, as demonstrated by Bohlmark et al. [13], who achieved an ionised percentage of 90 % of the sputtered Ti particles. For other widely used metals, including Cu, Al, Ta, etc., recent papers [11,13] have demonstrated that a highly ionised percentage may be obtained using HiPIMS. However, DeKoven et al. demonstrated that the C^+/C^0 ratio for carbon does not surpass 5 % when employing HiPIMS (by using Ar as the standard sputtering gas) [14]. This fact is due to the low carbon ionisation cross-section by electron impact.

Ganesan et al. [15] demonstrated that the utilization of the bipolar HiPIMS method improved the deposition rate of carbon films and elevated the sp^3 fraction to 45.4 %, which correlated with the identified compressive stress. This technique preserved the advantages of ionised deposition, potentially preventing the formation of arcs and the emission of macroparticles. The study found that the best combination of positive and negative pulse lengths (both set at 150 μs) resulted in heightened deposition rate, increased sp^3 fraction, and reduced argon content, comparable to DC magnetron sputtering. Films exhibiting these properties displayed a 50 % reduction in flank wear during machining, attributed to enhanced hardness and the optimization of pulse lengths. Santiago et al. also demonstrated that the HiPIMS method with positive voltage pulses enhances DLC coating quality [16]. Increased positive pulse voltage boosts ionisation, resulting in denser coatings, higher sp^3 content, and increased hardness up to 22.5 GPa.

On the other hand, Lin et al. produced DLC films using a variant of HiPIMS, called deep oscillation magnetron sputtering (DOMS), using variable deposition factors (substrate bias, pressure, current) [17]. Enhanced sp^3 bond formation, density, and smoothness were achieved with higher current and controlled bias.

The authors [18] have recently used the DOMS technique to produce DLC coatings in a Ne-rich discharge. They showed that a higher ionisation of carbon could be achieved by using Ne-DOMS discharge as compared to Ar-DOMS discharge. Because Ne has greater ionisation energy than Ar (21.56 vs 15.6 eV), adding Ne to the plasma raises the electron temperature, which in turn raises the ionisation fraction of the carbon species that is sputtered [19]. It was demonstrated that a higher ionisation of C facilitates the synthesis of denser and harder hydrogenated-free DLC films (hardness of DLC films up to 22 GPa was achieved). Regarding tribological performance, the DLC films had coefficient of friction values close to 0.15, i.e., within the range of typical values for DLC films tested in relatively humid conditions [20]. However, the use of DOMS to generate hydrogenated DLC films has not yet been investigated. Hydrogenated DLC films have better tribological performance than hydrogen-free DLC films depending on the humidity to which they are applied [21,22]. Additionally, hydrogenated DLC films often feature a hydrogen layer that contributes to further surface refinement, yielding an impressively low roughness of approximately 0.05 nm for films deposited on silicon substrates [23]. Moreover, hydrogenated DLC films display improved adhesion attributes due to diminished internal stress and enhanced interfacial bonding [6]. This characteristic is crucial for maintaining coating integrity in mechanically demanding situations.

The current study aims to investigate the viability of DOMS for producing hydrogenated DLC films in an argon-methane discharge gas and to identify the correlations between gas phase composition and mechanical properties of the produced films. This goal was achieved by sputtering a graphite target in an Ar-CH_4 ambient using different Ar-CH_4 compositions (from 0 % up to 10 % of CH4 in the Ar-CH4 mixture). SEM micrographics were taken to study the thickness and morphology, nanoindentation was made to evaluate the mechanical properties, pin-on-disk tests were run to evaluate the tribological properties (CoF and specific wear rate), and ion beam analysis (IBA) was carried out to determine the elemental composition of thin films synthesised in this study.

2. Experimental procedure

The DLC films were deposited on both Si (100) wafers with a dimension of 15 × 15 mm and AISI D2 cylindrical stainless steel (25 mm radius and 8 mm thickness) substrates. The latter were mirror polished beforehand by diamond paste (R_a = 0.3 μm). Both types of substrates were cleaned using an ultrasound bath of acetone and ethanol, for 15 min each. Then, they were glued to the sample-holder using an electric conductive glue and placed in the deposition chamber center, which was a high-grade steel cube with 400 mm edge length. The deposition chamber was equipped with two targets: the graphite one (99.95 %), which was needed to deposit the DLC layer, therefore, connected to the DOMS power supply (HiPIMS Cyprium™ plasma generator, Zpulser Inc.); and the chromium one (99.99 % purity), that was used to deposit an intermediate adhesion layer. Both have dimensions of 150 × 150 mm and 10 mm in thickness. The sample-holder rotates at 23.5 rpm, and it was kept at 80 mm from the targets. A base pressure, always lower than 2×10^{-3} Pa was obtained before every deposition. The adhesion interlayer was synthesised starting with a pure Ar atmosphere (0.8 Pa) at 1200 W and a substrate bias of −60 V. Then a Nitrogen gradient was introduced, to form a CrN interlayer. The overall thickness of this Cr/CrN interlayer was approximately 1 μm. The DLC layer was deposited in one hour using the DOMS source in the automatic mode: that is, the source voltage (DC_{int}), the constant voltage on time (t_{on}), the period (T), and the pulse duration (D) were set by the user to 400 V, 6 μs, 130 μs, and 1690 μs, respectively, while the pulse frequency was automatically adjusted to maintain an average power (P_a) of 1.3 kW. These parameters are represented in Fig. 1. The Ar and CH4 gas injection in the chamber was controlled by two separate mass flow controllers to adjust the [CH4]/[Ar + CH4] ratio to 0, 1.25, 2.5, 4.38, 6.25 or 10 % with the total flow rates of approximately 20 sccm while keeping the overall pressure in the chamber at 0.8 Pa. The values of the pulse voltage (V_p) and current (I_p), along with the pulse frequency (F_i) are given in Table 1 for the different Ar: CH4 gas mixtures. The pulse power (P_p) is defined as the V_p * I_p product.

The thin film composition was derived from Particle induced X-ray Emission (PIXE), Rutherford Backscattering Spectrometry (RBS) and Elastic Recoil Detection (ERD) measurements performed at the Synthesis, Irradiation and Analysis of Materials (SIAM) laboratory. RBS and PIXE were carried out in normal incidence, using an alpha beam at 4.3 MeV for sensitivity to carbon [24–27]. The backscattered particles were collected by 2 detectors set at 135° and 165° with respect to the incident beam direction. The sample was then tilted at 70° to be analysed with an alpha beam at 2.3 MeV for the hydrogen quantitation using a detector set at 30° relative to the incident beam direction. The set of 5 spectra acquired on each sample was self-consistently fitted with DataFurnace [28] (using the stopping power provided by SRIM database (www.srim.org) as well as the evaluated cross-section functions available on the SigmaCalc [29]) for extracting the elemental depth profiles [30]. To evaluate both surface and section morphologies, as well as the film thickness, SEM micrographs were taken. The equipment used was a Quanta 400FEG ESEM, using an acceleration voltage of 2 keV. The films' composition was also measured by Energy Dispersive X-ray Spectroscopy (EDS). The local structure of the DLC films was characterised by Raman spectroscopy using a blue/violet diode laser with a wavelength of 442 nm. Young's Modulus and Hardness were measured by depth-sensing indentation, using the MicroMaterials NanoTest platform with a Berkovich diamond indenter. A minimum of 14 measurements were performed, with a maximum load of 10 mN. The load was applied to ensure the indentation did not surpass 1/10 of the film thickness. Roughness results were performed from at least 3 AFM scans in Bruker

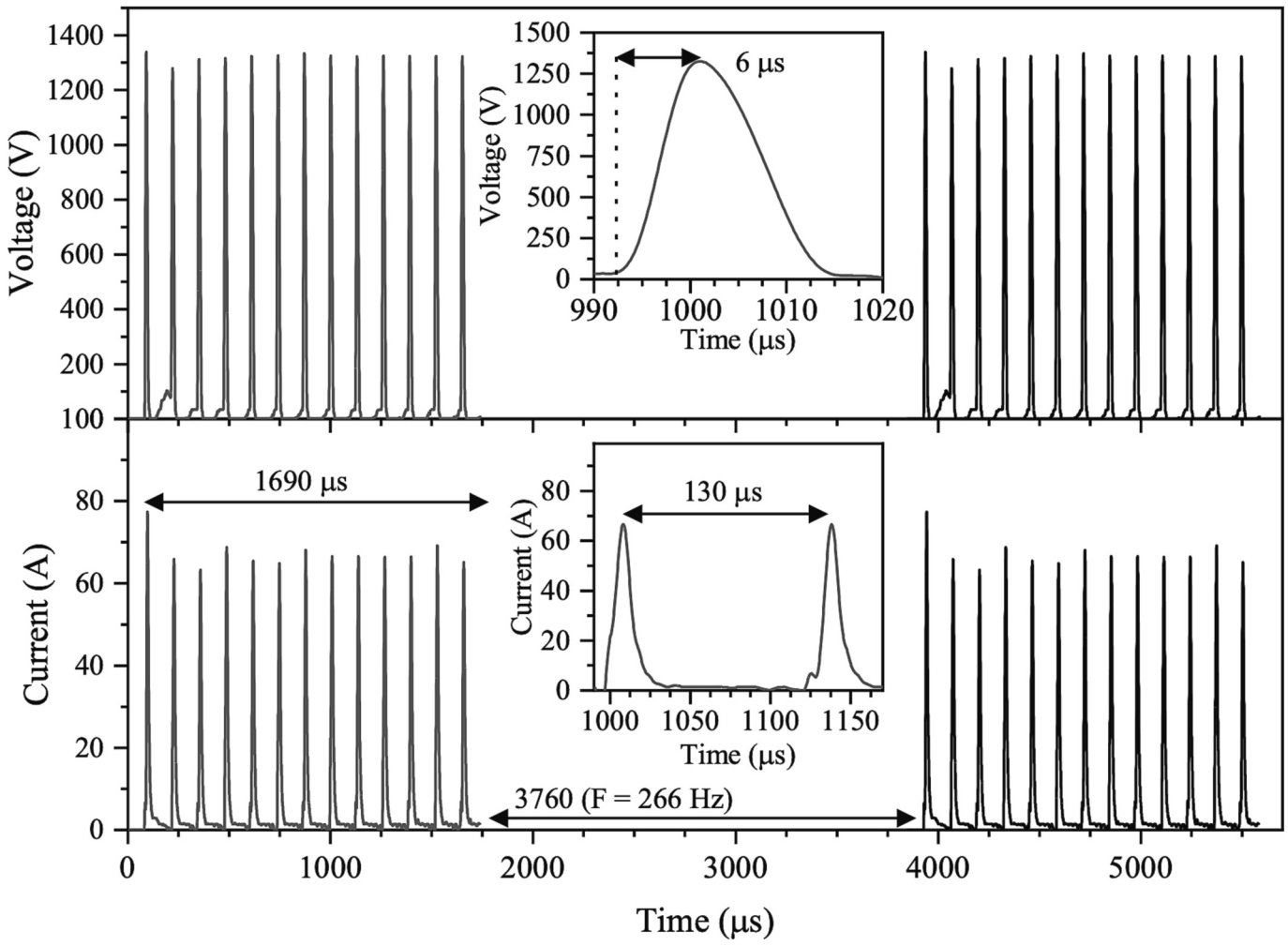

Fig. 1. DOMS impulse representing the different deposition parameters, (the diagrams in the middle represent an amplification of the impulse, allowing for a better view of the oscillations).

Table 1
Deposition conditions for DOMS with different methane percentages (P_a – average power; V_p – peak power; I_p – peak current; Pp – peak power; F_i – impulse frequency).

[CH4]/[Ar + CH4]	P_a	V_p	I_p	P_p	F_i	Thickness
(%)	(kW)	(V)	(A)	(kW)	Hz	nm
0	1.3	1386	79	110	263	711
1.25		1384	80	111	250	718
2.5		1383	81	112	256	767
4.38		1357	87	118	258	819
6.25		1340	90	121	266	908
10		1282	107	137	266	878

Innova AFM apparatus with 3 × 3 μm scan area in contact mode using silicon tip with less than 8 nm of tip radios. The mean roughness (Sa) value of height irregularities (sum of absolute values of data differences from the mean) was calculate from the collected data. The same measurement procedure was used for all the samples thus allowing for direct comparison of the results.

For evaluating the tribological performance, pin-on-disk tests were performed on the films deposited in the stainless-steel substrates. Those tests were conducted in an ambient atmosphere (room temperature and ~50 % relative humidity) using 10 mm AISI 52100 balls as counterparts. All tests (three-time repeats for each sample) were carried out for 160,000 cycles at a radius of 5 mm with a linear speed of 0.1 m/s, and 5 N load. The cross-section of the wear tracks created by the previous test was taken by a 2D profilometer, using the RituToyo Surf test SV-500, to obtain the wear volume, used in the calculation of the specific wear rate. Further details of the tribological tests performed in this study can be found elsewhere [18].

3. Results and discussion

Fig. 2 shows the RBS spectrum taken on the sample deposited in the Ar:CH4 mixture with [CH4]/[Ar + CH4] ratio of 1.25 % of methane. This spectrum nicely highlights the presence of the chromium interlayer (light green) with a gradient showing the progressive transition from pure Cr to Cr:N sublayers. It also shows the contribution of the carbon (light blue), as well as nitrogen (dark purple) and a small content of Ar (brown) within the DLC like layer (also confirmed by PIXE). Of course, hydrogen cannot be seen in backscattered particles, and therefore RBS has been complemented by ERD analysis (not shown here).

Fig. 3 shows the hydrogen concentration (derived from ERD; in at. %) contained in the different thin films as a function of the methane fraction within the Ar:CH4 mixture used for their synthesis. The trend clearly shows a sub-linear increase in hydrogen content with the increase in methane fraction within the Ar:CH4 mixture. This occurs due to a relative saturation of the carbon matrix of the DLC film, in relation to the hydrogen species [31]. The first film was deposited in an atmosphere free of methane, but still has 4.6 ± 0.2 at.% of hydrogen in its

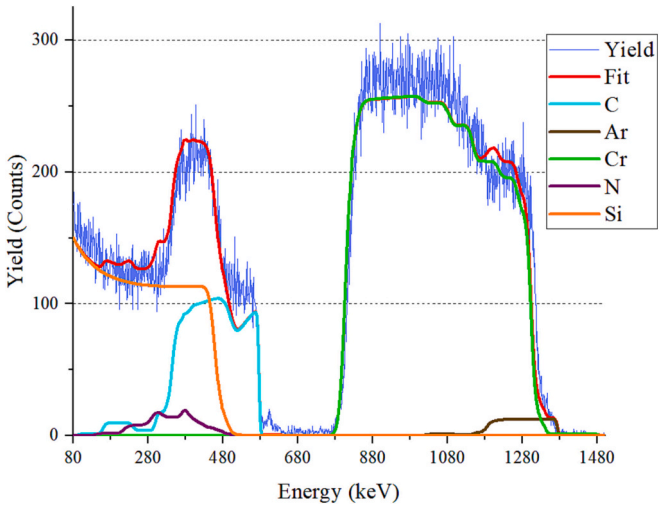

Fig. 2. RBS spectrum acquired at 4.3 MeV at 135° for the sample deposited with 1.25 % of [CH4]/[Ar + CH4] ratio in the Ar:CH4 mixture. The experimental spectrum is shown in light purple, while the red curve indicates the fitted spectrum. The latter comes from the contributions of the different elements contained in the sample: the silicon backing (orange), chromium (green), nitrogen (dark purple), carbon (light blue) and argon (brown).

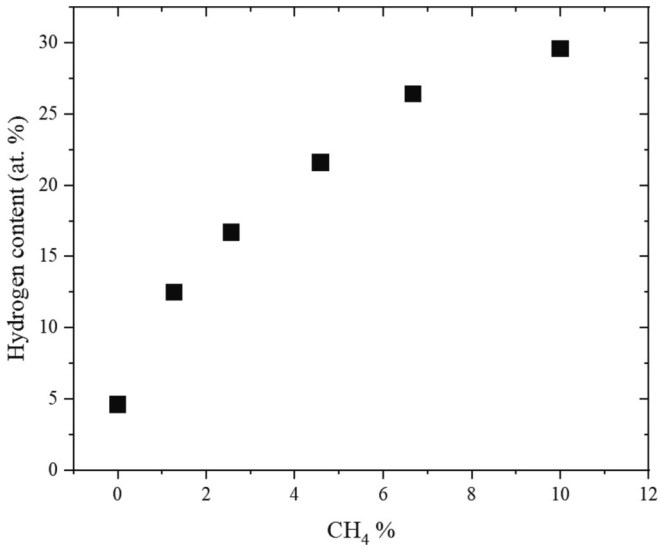

Fig. 3. Hydrogen content compared with the percentage of methane in the deposition chamber.

constitution. The small amount of H contained in this film is due to the moisture adsorbed on the inner walls of the deposition chamber. For the remaining samples, the content of hydrogen increases due to the increase of methane in the Ar/CH4 gas mixture, which leads to more hydrogen available for being incorporated in the DLC layer. The film deposited in [CH4]/[Ar + CH4] = 1.25 % gas mixture is made up of by 12.5 ± 0.4 at.% of hydrogen. The next three samples, deposited in [CH4]/[Ar + CH4] = 2.5 %, 4.38 % and 6.25 % have 16.7 ± 0.4, 21.6 ± 0.5 and 26.4 ± 0.6 at.% of hydrogen, respectively. The one deposited with the highest methane for this study has a concentration of hydrogen equal to 29.6 ± 0.9 at.%.

Fig. 4 represents the percentage of argon entrapped in the carbon matrix of the DLC films. The Ar incorporation is inevitable due to the bias voltage (−60 V) applied to the substrate during the deposition process, leading to the bombardment of the film by the Ar^+ ions available in the plasma [32]. The graph shows a clear reduction of the argon

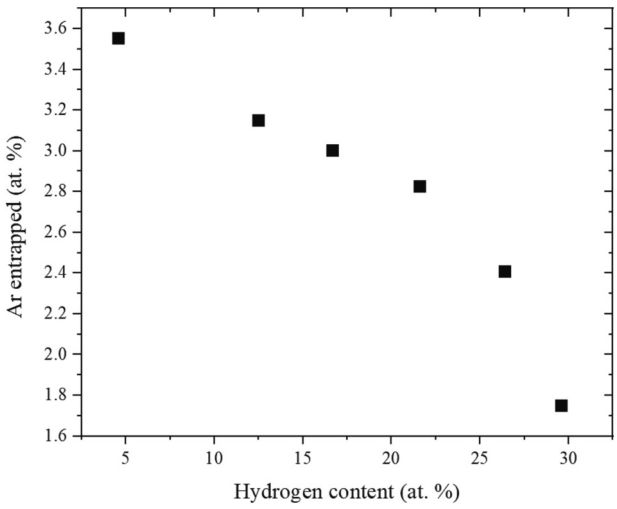

Fig. 4. Argon entrapped in the DLC matrix of the different films as a function of their hydrogen content.

species in the films composition. For the film deposited in pure Ar, the argon content is 3.5 ± 0.1 at.%, as for the film deposited in maximum methane, the argon presence is 1.7 ± 0.1 at.%. Therefore, a film deposited in 90 % argon and 10 % methane has half of the argon compared to the one deposited in 100 % argon. This happens as a result of the dissociation of the hydrocarbons in the plasma, which means a reduction of the argon proportion in the deposition chamber.

Table 2 summarizes the chemical composition of the deposited DLC films. All DLC films present small amounts of oxygen and nitrogen. Oxygen/nitrogen can be introduced into the films from various sources, such as residual gas in the deposition chamber, impurities in the target material, or from the substrate itself. Moreover, the DLC films' exposure to ambient air after deposition can lead to the adsorption of oxygen/nitrogen on the film's surface.

The SEM images are represented in Fig. 5. The cross-section of the films, revealing the microstructure of the different layers which their thickness measurements are shown. In image a) the 3 layers deposited are highlighted. First comes the pure chromium layer, followed by a Cr:N gradient that ends up in the chromium nitride layer. These two layers made up the interlayer that enhances the adhesion of the DLC film to the substrate. Both have a columnar microstructure, which is common for chromium films deposited by DCMS.

In images a), c), e), g), i) and j) the microstructure of the DLC layer is shown. This layer is dense in all samples. This kind of microstructure is normal for the substrate biasing and deposition pressures used in this study [33].

The images on the right in Fig. 5 show the surface of the DLC films. Unlike the previous images, these ones show differences between the various samples. The morphology of the surface of the film deposited in a methane free atmosphere is represented in image b) and is made up of by irregular aggregates of cauliflower-type shape, so common in films

Table 2
Chemical composition of the deposited DLC films.

[CH4]/[Ar + CH4]	C	H	N	O	Ar
(%)	at. %				
0	85.9 ± 0.5	4.6 ± 0.2	2.5 ± 0.1	3.5 ± 0.2	3.5 ± 0.1
1.25	79.7 ± 0.3	12.5 ± 0.4	1.7 ± 0.2	3.0 ± 0.3	3.1 ± 0.0
2.5	75.6 ± 0.1	16.7 ± 0.4	1.5 ± 0.1	3.2 ± 0.1	3.0 ± 0.0
4.38	71.1 ± 0.2	21.6 ± 0.5	1.8 ± 0.3	2.7 ± 0.3	2.8 ± 0.1
6.25	67.1 ± 0.4	26.4 ± 0.6	0.8 ± 0.1	3.6 ± 0.4	2.1 ± 0.2
10	64.6 ± 0.3	29.6 ± 0.9	1.2 ± 0.2	2.9 ± 0.2	1.7 ± 0.1

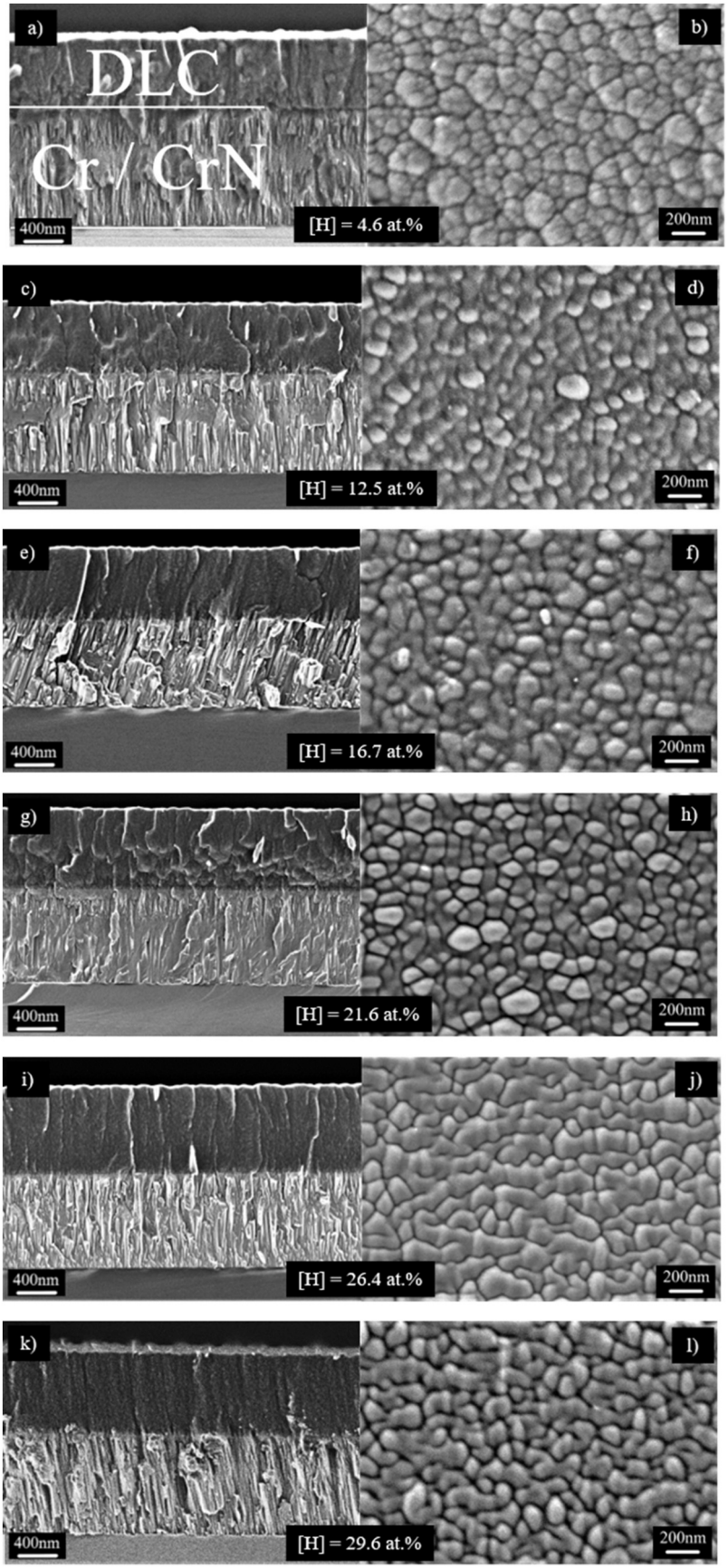

Fig. 5. Cross-sectional (left) and conventional (right) SEM micrographs for the samples synthesised in various Ar:CH4 gas mixtures (see Table 1).

deposited by magnetron sputtering under the influence of the atomic shadowing effect [18]. But the film deposited with the minimum percentage of methane ([CH4]/[Ar + CH4] = 1.25 %) has a different surface morphology and is made up of smooth and dense globular aggregates with compact boundaries. For the remaining samples of hydrogenated DLC, as the percentage of hydrogen increases, the surface is increasingly smoother, and the boundaries between those structures are almost disappeared. The micrographs j) and l) clearly show the tendency for smoother surfaces by increasing the hydrogen content. The reason behind these globular aggregates may be explained by the enhanced ion bombardment due to the hydrocarbon species. As seen in Table 1, the peak power increases with the methane fraction in the deposition chamber. This signifies a more potent ion bombardment, which leads to a smoother surface and globular features in the surface morphology. In the previous study, these features appeared by optimising the substrate bias and substituting Argon with Neon in the discharge gas, which enhanced the ion bombardment [18].

The cross-sectional SEM micrographs also gave the thickness of the layers for the different samples. And, as all the depositions had the duration of one hour, the rate was obtained directly. Fig. 6 presents the values of the deposition rates for all the samples. It is possible to see that the deposition rate increases with the hydrogen content. The rate starts with the value 11.8 nm/min for the film deposited in pure Ar and is not significantly affected by the introduction of [CH4]/[Ar + CH4] = 1.25 % in the gas discharge. Then it grows linearly with the increase of CH4 fraction in the Ar:CH4 gas mixture up to about 15 nm/min where it seems to reach a plateau (corresponding to about 7 % of CH4 in the gas mixture). In total, the increase of methane in the deposition chamber, allowed for a positive variation of 27 % of the deposition rate. As reported in the works of J. Lin et al., the hydrocarbon molecules (in this case, methane) dissociate in the plasma, and the resulting carbon species contribute to the film growth [30]. However, when the methane increases to 10 %, a decrease in the deposition rate is observed. The increased coverage of the graphite target racetrack with a hydrocarbon film at a very high methane fraction decreased the target sputter yield [33].

The Raman spectra of DLC films usually display at least two prominent peaks: the D peak, typically located at around 1350 cm-1, and the G peak, located at around 1580 cm-1. The intensity of the D peak is related to the amount of disorder and defects present in the DLC coating while that of the G peak is associated to the degree of graphitisation and the size of the graphitic domains present in the DLC coating [34]. Both peaks appear in the Raman spectra of the DLC films deposited in this study, as shown in Fig. 7 for the DLC films deposited with 1.25 % and 10 % a lower intensity peak, located close to 1200 cm^{-1}. A similar peak was reported by Boubiche et al. [35] for ta-C films deposited by PLD and Popov et al. [36] for ultra-nanocrystalline diamond films deposited by MWCVD. This peak has been labelled the "Nc" peak in this study as it is usually associated with the presence of nanocrystalline sp^3 domains in the DLC films. The fitting parameters obtained for the deconvolution of the Raman spectra shown in Fig. 7 are reported in Table 3.

The full width at half ~maximum (FWHM) of the G peak can provide information about the degree of disorder or defects in the DLC coating, as well as the size and number of graphitic domains [34]. Increasing the CH4 content in the plasma from 1.25 to 10 % resulted in a decrease of the FWHM of the G peak by more than 20 % (see Table 3). The smaller FWHM of the G peak of the DLC film with the highest H content indicates

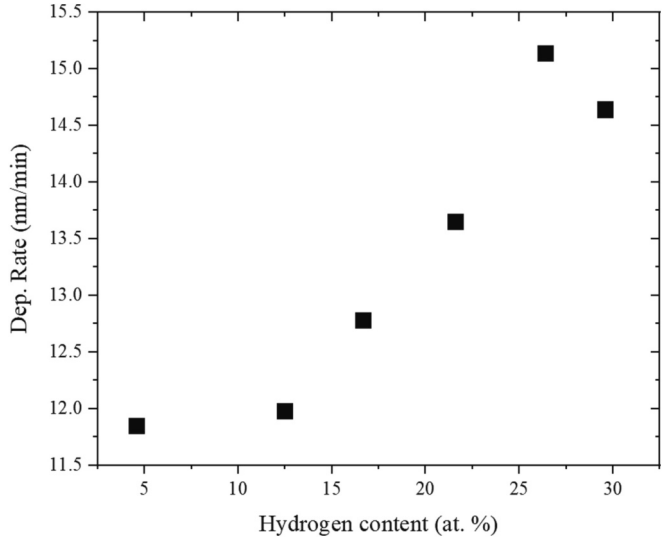

Fig. 6. Deposition rate of DLC films as a function of their hydrogen content (as measured by IBA).

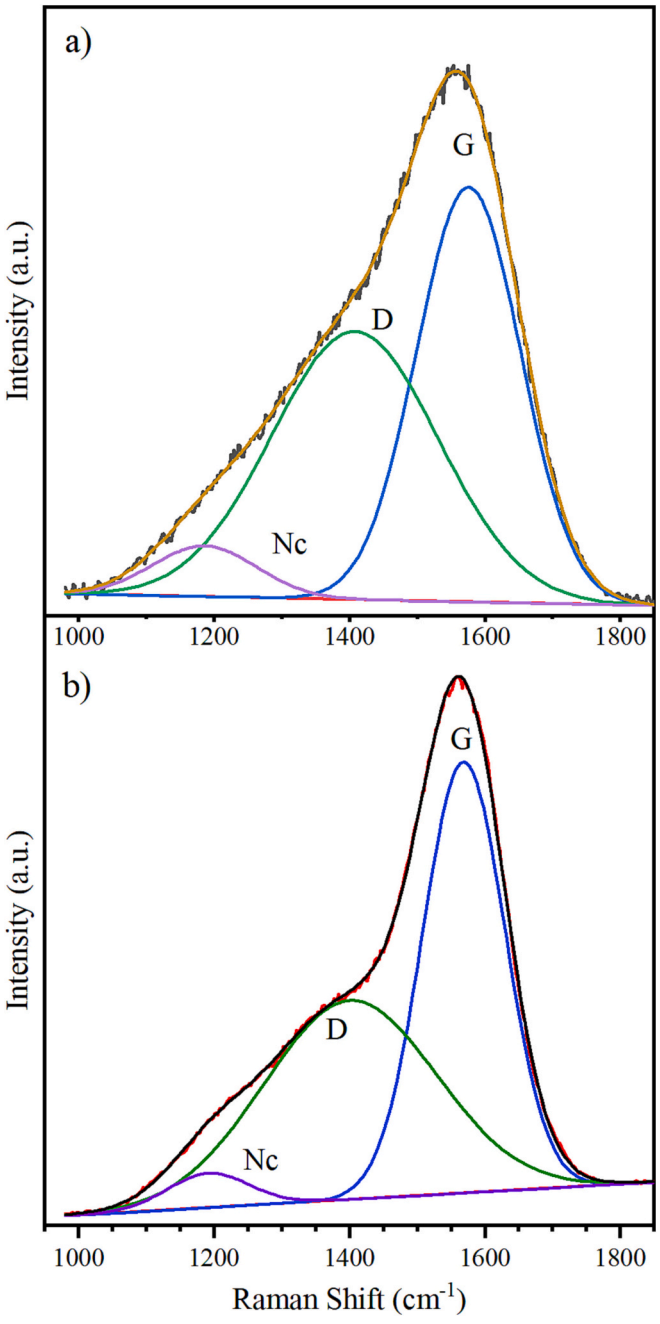

Fig. 7. Raman spectra of the DLC films deposited with a) 1.25 % and b) 10 % CH_4 in the plasma.

Table 3
Fitting parameters of the Raman spectra of the DLC films deposited with 1.25 and 10 % Ch_4 in the plasma.

[CH4]/[Ar + CH4] (%)		G peak	D peak	Nc peak
1.25	Position (cm^{-1}):	1576	1407	1196
	FWHM (cm^{-1}):	180	270	186
	Intensity (a.u.):	120,856	111,876	17,629
10	Position (cm^{-1}):	1569	1401	1191
	FWHM (cm^{-1}):	143	299	142
	Intensity (a.u.):	545,179	524,553	42,834

less disorder and greater sized sp^2 domains and, thus, a lower sp^3 content. On the other hand, Omarov et al. [37] showed that the $I_{Nc}/(I_D + I_G)$ intensity ratio was proportional to the fraction of the sp^3 bonded carbon atoms in DLC-coatings synthesised in RF discharge. In this study, increasing the CH_4 content in the plasma from 1.25 % to 10 % resulted in a decrease of the INc/(ID+IG) ratio from 7.0 to 3.8 %, i.e., a reduction by almost 50 %. Thus, adding CH_4 to the plasma significantly decreased the sp^3 content of the DLC films.

The hardness and Young's Modulus of the films obtained by the nanoindentation test are presented in Fig. 8. Comparing the first two values, although the error bars do not allow for a clear conclusion, the data shows an improvement of the mechanical properties with a minimal introduction of CH_4 in the deposition chamber (4.6 ± 0.2 at. % hydrogen content), from 20 GPa to 23 GPa. This slight variation may be due to the enhanced ion bombardment, also referred to as the reason for the globular aggregates taken by the SEM superficial micrographs. This ion bombardment increases the density of the film, increasing its hardness. However, from 4.6 ± 0.2 at. % onwards, the mechanical properties decrease gradually with higher hydrogen content. Decreasing to 20 GPa, for the film with 16.7 ± 0.4 at. % of hydrogen, then to 18 GPa and 13 GPa for 21.6 ± 0.5 and 26.4 ± 0.6 at.% of hydrogen, respectively. The minimum hardness value obtained is 11 GPa for the sample deposited with higher methane content (29.6 ± 0.9 at. %). As shown by Raman spectroscopy, the hydrogen atoms break the carbon network, reducing the C—C sp^3 links, which determine the mechanical properties of the carbon films [2,6,32].

The values of the coefficient of friction (CoF) during the tribological tests are represented in Fig. 9. None of the samples failed during the 160,000 cycles of the pin-on-disk test. All lines of the CoF produced by that test have all a clear running in period, and a stable period, although the test with 4.6 ± 0.2 at. % of H (the one deposited in pure Ar) took much longer to achieve the last stage. By cycle 140,000 all samples reached the steady stage, where a constant value was taken. Those

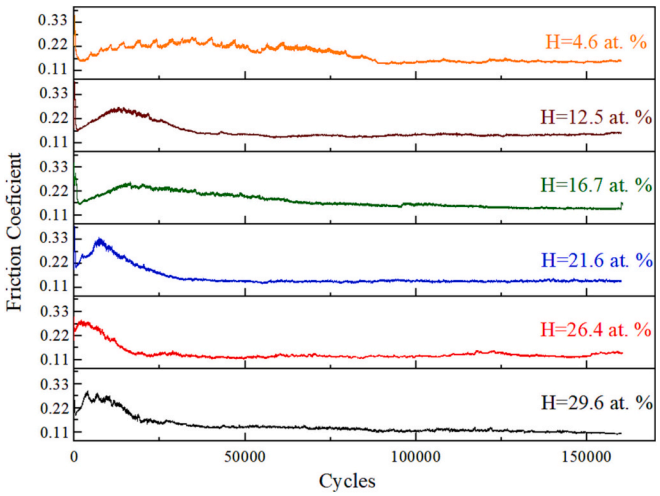

Fig. 9. Coefficient of friction during the pin-on-disk tests.

values are represented in Fig. 10. All the values are beneath 0.16 which is normal for non-doped DLC in relative humid conditions [7,38]. The average CoF for the two first samples (4.6 ± 0.2 at.% and 12.5 ± 0.4 at. % of hydrogen) have similar values, around 0.15. This value decreases to about 0.14 for the next two samples. For the sample with 26.4 ± 0.6 at. % of hydrogen, the CoF slightly decreases to about 0.13. And finally, for the sample with the most hydrogen the CoF has its lower value, 0.11. Overall, the coefficient of friction decreases by 30 % from the film with almost no hydrogen to the film with almost one third of it. The fact that all the films have such low CoF is due to the formation of a transfer layer between the two moving surfaces [39]. That layer was created either by the transformation of sp3 bonding to sp2 bonding or structural modifications of sp2 sites by the friction heat, originating graphite, which is known for its great tribological properties [8]. In all the sliding tests conducted within this study, a transfer layer consistently developed on the spherical counterpart, as exemplified in Fig. 11 for the film containing 16.7 at. % of hydrogen. Correspondingly, an Energy Dispersive Spectroscopy (EDS) examination conducted on the counterpart disclosed a blend of carbon originating from the DLC films and oxidized metallic components from the counterpart. This is visually depicted in the supplementary EDS insert within Fig. 11. The reduction of the CoF as the hydrogen content increase can also be explained by the decrease in surface roughness (surface roughness measured by AFM, see Table 4). As

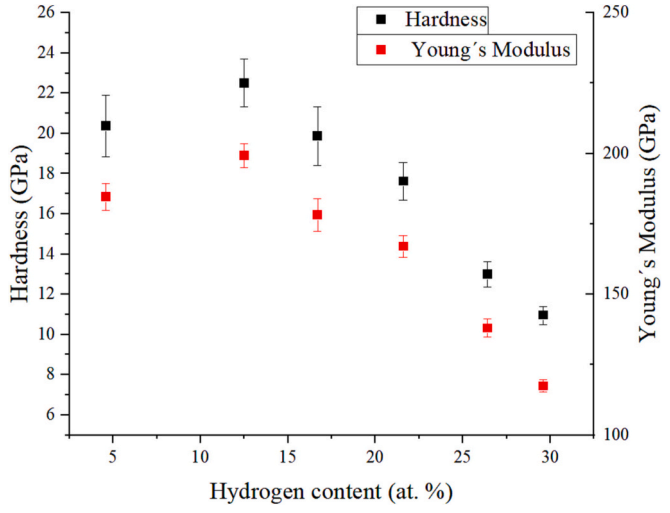

Fig. 8. Hardness and Young's modulus of the DLC coatings as a function of the hydrogen content.

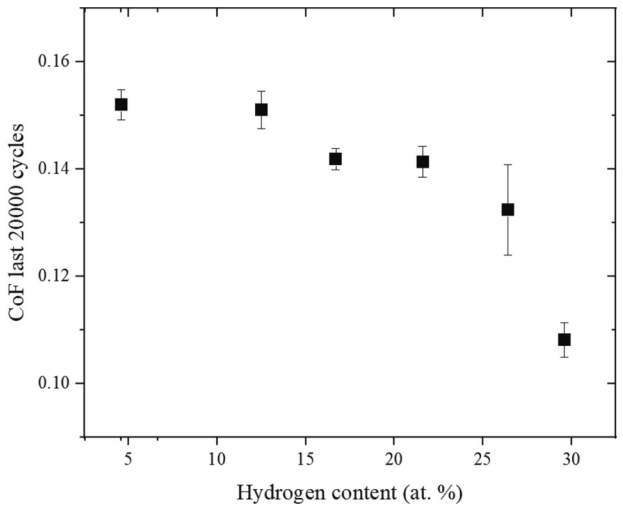

Fig. 10. Average coefficient of friction for the last 20,000 cycles of the pin-on-disk test as a function of hydrogen content.

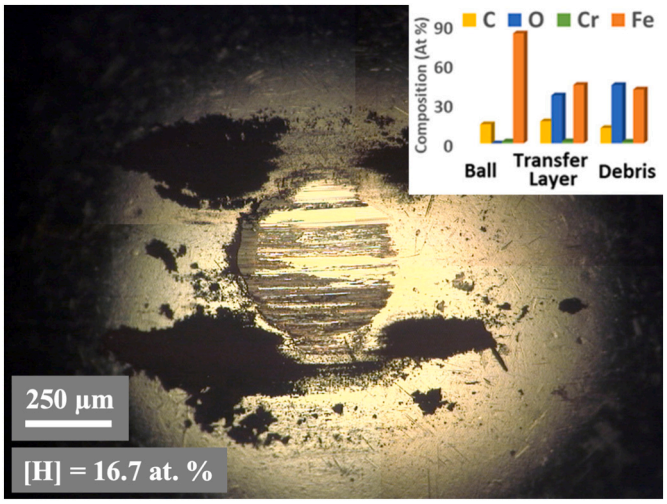

Fig. 11. Typical transfer layer formed on the ball counterpart during pin-on-disk tests (magnification: 5×). The insert presents EDS elementary composition graph for the different ball areas: transfer layer; ball and debris.

Table 4
Roughness of the deposited DLC films.

[CH4]/ [Ar + CH4] (%)	Roughness (nm)
0	8 ± 0.3
1.25	7.5 ± 0.4
2.5	5.5 ± 0.5
4.38	5.3 ± 0.3
6.25	4 ± 0.4
10	3.5 ± 0.3

was explained earlier, the surface of the films with the most hydrogen in its composition, have the flattest surface aggregates, which makes their surface the smoothest. This could explain why these films have the lowest CoF. On the other hand, the influence of hydrogen in the tribological behaviour of a DLC film is very complex and depends on the environment in which the test is run. In an inert environment, hydrogenated DLC has a much lower coefficient of friction than its hydrogen free counterpart. However, when the test is made in a normal ambient, the difference between the coefficients is not that high. As there is humidity in the air, the hydrogen free DLC decreases its CoF, but it increases for hydrogenated DLC [21,38].

Fig. 12 represents the 2D profiles of the wear tracks taken in the profilometer. Before the determination of the specific wear rate, it is possible to see that the wear tracks increase with the more hydrogenated DLC films, both in depth and in width. With the area of those tracks, the specific wear rate was calculated, and the results are shown in Fig. 13. It is possible to see that the wear rate rises with the hydrogen content,

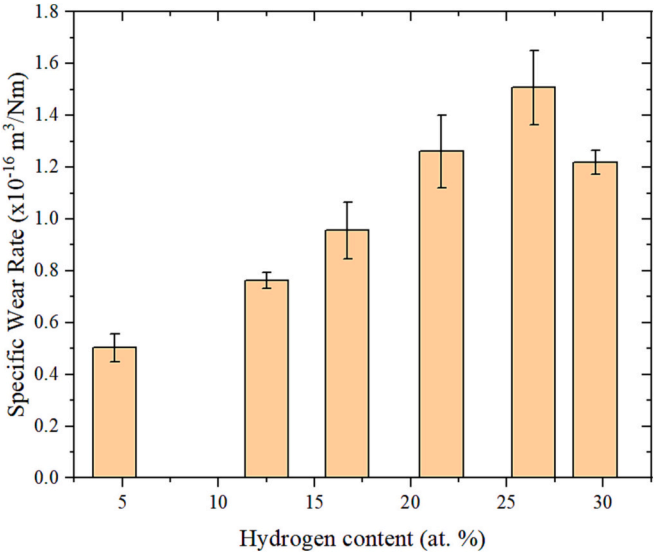

Fig. 13. Specific wear rates of the DLC films as a function of the hydrogen content.

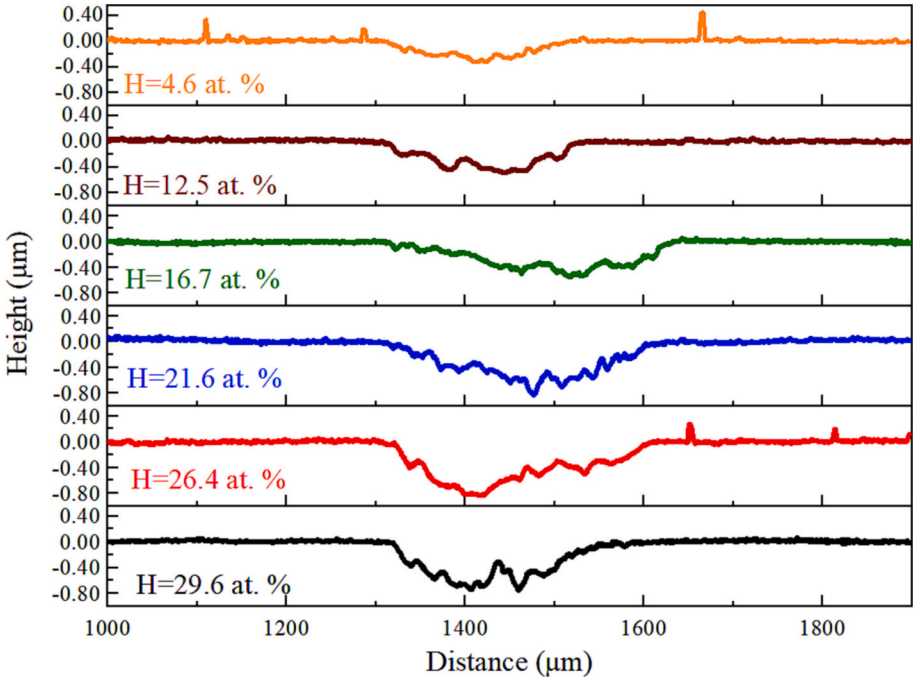

Fig. 12. 2D profiles of the wear tracks of the DLC films created during the pin-on-disk tests.

except in the last sample (29.6 ± 0.9 at. %). The minimum value for this tribological property is 0.50 × 10^{-16} m^3/Nm (0.50 × 10^{-7} mm^3/Nm) for the film with 4.6 ± 0.2 at. % of hydrogen, and its maximum is 1.51 × 10^{-16} m^3/Nm (1.51 × 10^{-7} mm^3/Nm) for the film with 26.4 ± 0.4 at.% of hydrogen. The wear rate values obtained for all the samples are within the usual window for hydrogenated DLC films (around 10^{-6} mm^3/Nm and 10^{-7} mm^3/Nm) [2,40]. This variation represents a variation of 200 % of the wear rate, which is quite significant. The upward tendency observed confirms the hypothesis created in the analysis of the wear tracks profiles.

The tendency of a higher specific wear rate with higher hydrogen content can be compared with the hardness variation shown before. In this one, although the error bars are quite large, it is possible to see a clear decrease of the hardness with increasing hydrogen content. In the case of the wear rate, the exact opposite happens. The wear rate is minimum for the film with 4.6 ± 0.2 at. % of hydrogen and increases as the hydrogen content also increases (except in the last sample, which is also harder than the 26.4 % ± 0.6 at.). This correlation can be explained by the Archard's equation, which states that the wear rate of a determined surface is inversely proportional to its hardness [2].

4. Conclusion

In this study, hydrogenated DLC films were deposited using the HiPIMS-DOMS method by using different Ar:CH4 gas mixtures for the deposition process. This variation allowed the deposition of films with increasingly more hydrogen content, reaching approximately 30 at. % for the film synthesised from a gas mixture with 10 % of methane. The cross-sectional SEM micrographs showed a featureless cross-section morphology across all films. The superficial images taken by the same instrument showed a transformation from a cauliflower shape aggregate for the film with less hydrogen, to globular shaped aggregates that became increasingly smoother and flatter as the hydrogen content grows. The deposition rate is increasingly higher with more hydrogen. This is due to the dissociation of the methane molecules in the deposition chamber, where the carbon particles participate in the growing process of the film. Mechanically, the films with more hydrogen are softer than the ones with less hydrogen. Varying the content of hydrogen, induces a variation of approximately 50 % between the minimum and the maximum value. The coefficient of friction has the same tendency, as the film with less hydrogen has 0.15 and the richer one has 0.10. On the other hand, the specific wear rate has the opposite tendency, as the first film has 0.50 × 10^{-16} m^3/Nm, and the film with 26.4 at. % of H (the second film with more hydrogen), has 1.51 × 10^{-16} m^3/Nm.

Overall, this study showed a clear increase in the deposition rate with hydrogen content, which is very advantageous for uses in industry. Moreover, the coefficient of friction decreases from 0.15 to 0.10 with a higher hydrogen presence. This represents a clear benefit in relation to lowering friction losses. However, due to less hardness, the wear rate of the film increased by increasing the hydrogen content in the films, even though the value of the wear rate for all the samples is under 1.5 × 10^{-16} m^3/Nm, which is extremely low.

CRediT authorship contribution statement

All authors have given their approval to the final version of the manuscript.

Author Contribution Form.

All authors must check* the relevant terms to indicate their contributions. To know more about the CReDiT Author Statement and definitions of each term mentioned in the below form, please visit https://www.elsevier.com/authors/policies-and-guidelines/credit-author-statement

André Costa: Formal analysis, Investigation, Validation, Writing - Original draft preparation; **Fábio Ferreira**: Writing - Review & Editing, Supervision; **Julien** L. **Colaux**: Visualization, Investigation, Resources; ***Alireza Vahidi:*** Visualization, Investigation; **Ricardo Serra:** Validation; **João Oliveira:** Writing- Reviewing and Editing, Supervision, Project administration, Funding acquisition.

Declaration of competing interest

The authors declare that they have no known competing financial interests or personal relationships that could have appeared to influence the work reported in this paper.

Data availability

Data will be made available on request.

Acknowledgements

This research was funded by FEDER funds through COMPETE – Programa Operacional Factores de Competitividade – Programe, and by national funds through FCT – Fundação para a Ciência e a Tecnologia, under the project UIDB/00285/2020. This project has received funding from the European Union's Horizon 2020 research and innovation programme under grant agreement No 101007417, having benefited from the access provided by the University of Namur in Namur Institute of Structured Matter within the framework of the NFFA-Europe Pilot Transnational Access Activity, proposal ID038.

References

[1] K. Holmberg, P. Andersson, A. Erdemir, Global energy consumption due to friction in passenger cars, Tribol. Int. 47 (2012) 221–234.
[2] J. Robertson, Diamond-like amorphous carbon, Mater. Sci. Eng. R Rep. 37 (2002) 129–281.
[3] J. Vetter, 60years of DLC coatings: historical highlights and technical review of cathodic arc processes to synthesize various DLC types, and their evolution for industrial applications, Surf. Coat. Technol. 257 (2014) 213–240.
[4] A. Erdemir, J.M. Martin, Superior wear resistance of diamond and DLC coatings, Curr. Opin. Solid State Mater. Sci. 22 (2018) 243–254.
[5] A.W. Zia, M. Birkett, Deposition of diamond-like carbon coatings: conventional to non-conventional approaches for emerging markets, Ceram. Int. 47 (2021) 28075–28085.
[6] A. Grill, Diamond-like carbon: state of the art, Diam. Relat. Mater. 8 (1999) 428–434.
[7] A. Erdemir, C. Donnet, Tribology of diamond-like carbon films: recent progress and future prospects, J. Phys. D. Appl. Phys. 39 (2006) R311.
[8] Y. Liu, A. Erdemir, E.I. Meletis, A study of the wear mechanism of diamond-like carbon films, Surf. Coat. Technol. 82 (1996) 48–56.

[9] Y. Lifshitz, Diamond-like carbon—present status, Diam. Relat. Mater. 8 (1999) 1659–1676.
[10] Y. Lifshitz, Hydrogen-free amorphous carbon films: correlation between growth conditions and properties, Diam. Relat. Mater. 5 (1996) 388–400.
[11] U. Helmersson, M. Lattemann, J. Bohlmark, A.P. Ehiasarian, J.T. Gudmundsson, Ionized physical vapor deposition (IPVD): a review of technology and applications, Thin Solid Films 513 (2006) 1–24.
[12] V. Kouznetsov, K. Macak, J.M. Schneider, U. Helmersson, I. Petrov, A novel pulsed magnetron sputter technique utilizing very high target power densities, Surf. Coat. Technol. 122 (1999) 290–293.
[13] J. Bohlmark, J. Alami, C. Christou, A.P. Ehiasarian, U. Helmersson, Ionization of sputtered metals in high power pulsed magnetron sputtering, J. Vac. Sci. Technol. A 23 (2005) 18–22.
[14] B.M. Dekoven, P.R. Ward, R.E. Weiss, Advanced Energy Industries, F, Collins and A. Anders, L. Berkeley, 2003.
[15] R. Ganesan, I. Fernandez-Martinez, B. Akhavan, D.T.A. Matthews, D. Sergachev, M. Stueber, D.R. McKenzie, M.M.M. Bilek, Pulse length selection in bipolar HiPIMS for high deposition rate of smooth, hard amorphous carbon films, Surf. Coat. Technol. 454 (2023).
[16] J.A. Santiago, I. Fernández-Martínez, T. Kozák, J. Capek, A. Wennberg, J. M. Molina-Aldareguia, V. Bellido-González, R. González-Arrabal, M.A. Monclús, The influence of positive pulses on HiPIMS deposition of hard DLC coatings, Surf. Coat. Technol. 358 (2019) 43–49.
[17] J. Lin, W.D. Sproul, R. Wei, R. Chistyakov, Diamond like carbon films deposited by HiPIMS using oscillatory voltage pulses, Surf. Coat. Technol. 258 (2014) 1212–1222.
[18] F. Ferreira, R. Serra, A. Cavaleiro, J. Oliveira, Diamond-like carbon coatings deposited by deep oscillation magnetron sputtering in Ar-Ne discharges, Diam. Relat. Mater. 98 (2019), 107521.
[19] A. Aijaz, K. Sarakinos, D. Lundin, N. Brenning, U. Helmersson, A strategy for increased carbon ionization in magnetron sputtering discharges, Diam. Relat. Mater. 23 (2012) 1–4, https://doi.org/10.1016/j.diamond.2011.12.043.
[20] H. Ronkainen, K. Holmberg, Environmental and Thermal Effects on the Tribological Performance of DLC Coatings, Tribology of Diamond-like Carbon Films: Fundamentals and Applications, 2008, pp. 155–200.
[21] A. Erdemir, The role of hydrogen in tribological properties of diamond-like carbon films, Surf. Coat. Technol. 146 (2001) 292–297.
[22] E.R. Sivakumar, P. Senthilkumar, M. Sreenivasan, R. Krishna, Experimental investigation of H-DLC coated exhaust valve characteristics of a diesel engine, Mater. Today Proc. 33 (2020) 675–681.
[23] M. Roy, Chapter 8 - protective hard coatings for Tribological applications, in: A. K. Tyagi, S. Banerjee (Eds.), Materials Under Extreme Conditions, Elsevier, Amsterdam, 2017, pp. 259–292.
[24] A.F. Gurbich, Evaluation of non-Rutherford proton elastic scattering cross section for carbon, Nucl. Instrum. Methods Phys. Res. B 136 (1998) 60–65.
[25] N.P. Barradas, C. Jeynes, R.P. Webb, Simulated annealing analysis of Rutherford backscattering data, Appl. Phys. Lett. 71 (1997) 291–293.
[26] A.F. Gurbich, SigmaCalc recent development and present status of the evaluated cross-sections for IBA, Nucl. Instrum. Methods Phys. Res. B 371 (2016) 27–32.
[27] X. Zhou, S. Tunmee, T. Suzuki, P. Phothongkam, K. Kanda, K. Komatsu, S. Kawahara, H. Ito, H. Saitoh, Quantitative NEXAFS and solid-state NMR studies of sp3/(sp2+ sp3) ratio in the hydrogenated DLC films, Diam. Relat. Mater. 73 (2017) 232–240.
[28] D. Thiry, A. De Vreese, F. Renaux, J.L. Colaux, S. Lucas, Y. Guinet, L. Paccou, E. Bousser, R. Snyders, Toward a better understanding of the influence of the hydrocarbon precursor on the mechanical properties of a-C: H coatings synthesized by a hybrid PECVD/PVD method, Plasma Process. Polym. 13 (2016) 316–323.
[29] E. Mounier, Y. Pauleau, Mechanisms of intrinsic stress generation in amorphous carbon thin films prepared by magnetron sputtering, Diam. Relat. Mater. 6 (1997) 1182–1191.
[30] J. Lin, X. Zhang, P. Lee, R. Wei, Thick diamond like carbon coatings deposited by deep oscillation magnetron sputtering, Surf. Coat. Technol. 315 (2017) 294–302.
[31] G.A. Viana, E.F. Motta, M. Da Costa, F.L. Freire Jr., F.C. Marques, Diamond-like carbon deposited by plasma technique as a function of methane flow rate, Diam. Relat. Mater. 19 (2010) 756–759.
[32] J. Robertson, The deposition mechanism of diamond-like aC and aC: H, Diam. Relat. Mater. 3 (1994) 361–368.
[33] J. Robertson, Plasma deposition of diamond-like carbon, Jpn. J. Appl. Phys. 50 (2011) 01AF01.
[34] C. Casiraghi, A.C. Ferrari, J. Robertson, Raman spectroscopy of hydrogenated amorphous carbons, Phys. Rev. B 72 (2005), 085401.
[35] N. Boubiche, J. El Hamouchi, J. Hulik, M. Abdesslam, C. Speisser, F. Djeffal, F. Le Normand, Kinetics of graphitization of thin diamond-like carbon (DLC) films catalyzed by transition metal, Diam. Relat. Mater. 91 (2019) 190–198.
[36] C. Popov, W. Kulisch, P.N. Gibson, G. Ceccone, M. Jelinek, Growth and characterization of nanocrystalline diamond/amorphous carbon composite films prepared by MWCVD, Diam. Relat. Mater. 13 (2004) 1371–1376.
[37] A. Omarov, A. Kalinichenko, V. Strel'nitskij, I. Nasieka, I. Danylenko, M. Boyko, T. Sabov, The influence of different ratio of Ar and CH66 gases and ion bombardment on the growth rate and sp3 bonds content in DLC-coatings synthesized in RF discharge, Phys. Lett. A 443 (2022), 128221.
[38] K.A.H. Al Mahmud, M.A. Kalam, H.H. Masjuki, H.M. Mobarak, N.W.M. Zulkifli, An updated overview of diamond-like carbon coating in tribology, Crit. Rev. Solid State Mater. Sci. 40 (2015) 90–118.
[39] J.P. Hirvonen, R. Lappalainen, J. Koskinen, A. Anttila, T.R. Jervis, M. Trkula, Tribological characteristics of diamond-like films deposited with an arc-discharge method, J. Mater. Res. 5 (1990) 2524–2530.
[40] A.A. Voevodin, M.S. Donley, J.S. Zabinski, Pulsed laser deposition of diamond-like carbon wear protective coatings: a review, Surf. Coat. Technol. 92 (1997) 42–49.